University of Nairobi

Institute of Nuclear Science and Technology

RADIOLOGICAL HAZARD ASSESSMENT AND INVESTIGATION OF HEAVY MINERALS OF ECONOMIC IMPORTANCE IN MWITA SYANO RIVER BED SANDS.

By

Midigo Benard Odhiambo

BSc (Hons)

A thesis submitted in partial fulfilment for the degree of Master of Science in Nuclear Science of the University of Nairobi.

© 2015

DECLARATION

This thesis is my original work and has not been presented for a degree in any other university.

Signature…………………………. Date……………………

Midigo Benard Odhiambo

S56/74423/2012

This thesis has been submitted for examination with the knowledge of the supervisors

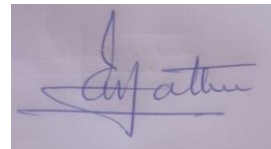Mr David Maina

Institute of Nuclear Science and Technology

University of Nairobi

Sign……………………

Date…9–11–2015

Prof. Eliud Mathu

Department of Geological Sciences

South Eastern Kenya University

Date……………………..

Prof. Michael Gatari Sign……………………

Institute of Nuclear Science and Technology Date……………………..

University of Nairobi

DEDICATION

I dedicate this work to my family members, friends, and my lecturers.

ACKNOWLEDGEMENT

ABSTRACT

Heavy minerals are important economic resources as they are useful in many industrial applications such as manufacturing of tiles and pigments. Even though heavy minerals are of great value, studies have shown that some minerals such as monazite which contain thorium, a radioactive element, and therefore heavy minerals may be a source of gamma radiation. Therefore, the main aim of this research was to investigate heavy minerals of economic importance and also to assess radiological impact of the heavy mineral sands in Mwita Syano River bed sands. The radiological impact was investigated using high purity germanium spectrometer while heavy mineral assessment was analysedusing X-ray Powder Diffraction spectrometer. The result showed that the activity concentration of ^{226}Ra varied between 4.52 Bq kg^{-1} and 35.7 Bq kg^{-1} with an average of 13.45 Bq kg^{-1} while ^{238}U ranged from 3.12 Bq kg^{-1} to 47.3 Bq kg^{-1} with an average of 8.12 Bq kg^{-1}. Specific activity of ^{40}K on the other hand varied between 111 Bq kg^{-1} and 459 Bq kg^{-1} with an average of 321 Bq kg^{-1} while the annual effective dose ranged between 0.0136-0.0787 mSv yr^{-1} with a mean of 0.031 mSv yr^{-1}. On the other hand XRD analysis showed that the only available heavy mineral of economic importance is magnetite which had an average percentage of 0.15 %. However, other valuable minerals such as albite and orthoclase were also found in the sands and they had an average percentage of 23.46 % and 4.67 % respectively. In conclusion therefore, the average specific activity of these sands are below the World averages hence they are not of radiological concern. The presence of magnetite, albite and orthoclase minerals indicate that there is a possibility that other heavy minerals could be present and therefore further analysis should be done on these sands. This is because heavy minerals are dense and therefore there is a possibility that they could have settled deeper into the ground.

Contents

LIST OF ABBREVIATION

ANL: Argonne National Laboratory

ASTM: American Standard of Testing of Materials

EDXRF: Energy Dispersive X-ray Fluorescence

G.P.S: Global Positioning System

HMS: Heavy Mineral Sand

HPGe: High Purity Germanium

NORM: Natural Occurring Radioactive Material

NSW: New South Wale

XRF: X-ray Fluorescence

XRD: X-ray powder Diffraction

List of Figures

List of Tables

Chapter 1

Introduction

1.0 Background Information

There has been increasing interests in identifying areas which are exposed to naturally occurring radioactive materials (NORM) around the world. This is because human beings and animals living in such areas may get exposed to high levels of radiation which are a health hazard. The natural radiation originates mainly from the primordial radionuclides (terrestrial background radiation) and cosmogenic radionuclides. Primordial radionuclides are long lived radionuclides with half-lives almost the same as the age of the earth (4.5 billion years) and therefore they can be found in different geological materials. Some of these primordial radionuclides are ^{238}U ($t_{1/2}$=4.47*10^9 years), ^{232}Th ($t_{1/2}$ $_=$1.41*10^9 years), and also ^{40}K ($t_{1/2=}$1.21*10^9 years) and their decay products. Cosmogenic radionuclides on the other hand are mainly produced by the interaction of cosmic rays with atomic nuclei in the atmosphere through nucleons synthesis (UNSCEAR, 2012). Gamma radiations from these radionuclides represent the main source of external radiation and therefore are considered as the main contributor of natural radiation (UNSCEAR, 2012). According to Veiga et al. (2006), one of the main sources of gamma radiation are the heavy mineral sands.

In a study done on four Brazilian beaches by Veiga et al. (2006), some of the beaches were found to be radiologically harmful. For example, the average radium equivalent was found to be 83,425 Bq kg^{-1} in Guarapari and 10205 Bq kg^{-1}in Meaipe. These values are far above 370 Bq kg^{-1} which has been recommended by NEA-OECD (1979) for the safe use of building materials.

Heavy mineral sand deposits are defined as loose aggregate of mineral or rock particles forming an unconsolidated or moderately consolidated sedimentary deposit consisting essentially of medium grained particles (Farooq et al., 2010). Typically they have specific gravity greater than 2.9 g cm^{-3} (NSW, 2007) and contain ^{238}U and ^{232}Th which

are radioactive. Though potentially radioactive, some heavy minerals are of great economic importance.

Heavy minerals consists of compounds which have a wide range of industrial applications. For example, ilmenite, rutile and leucoxene contain TiO_2 which is generally used in the manufacturing of white pigment among other products. Zircon is made up of $ZrSiO_4$, which is used in the ceramic industries. As a result the demand for zircon and titanium dioxide has gone up (GMP, 2011) and currently there is a widening gap between the supply and demand of these minerals because the supply cannot meet the market demand of the minerals. In fact GMP (2011) is forecasting "a shortage of ilmenite over the next two years, followed by a period of reasonable balance and then an emerging shortage from 2015, providing all near term new projects come into production on schedule" (Fig. 1.1). Therefore, several countries such as Australia, Canada, India, Kenya, Madagascar, Mozambique, and South Africa have started carrying major exploration of these sands (Pincock, 2005). In Kenya it is carried out in Kwale by Base Titanium Co. Ltd.

In this connection, this research was designed to investigate radioactivity as well as the heavy mineral composition of Mwita Syano River bed sands. Mwita Syano River was selected for this study because during pre-visit to the river, a magnet was used to test the presence of heavy minerals and from that test several sand crystals got attracted to the magnet.
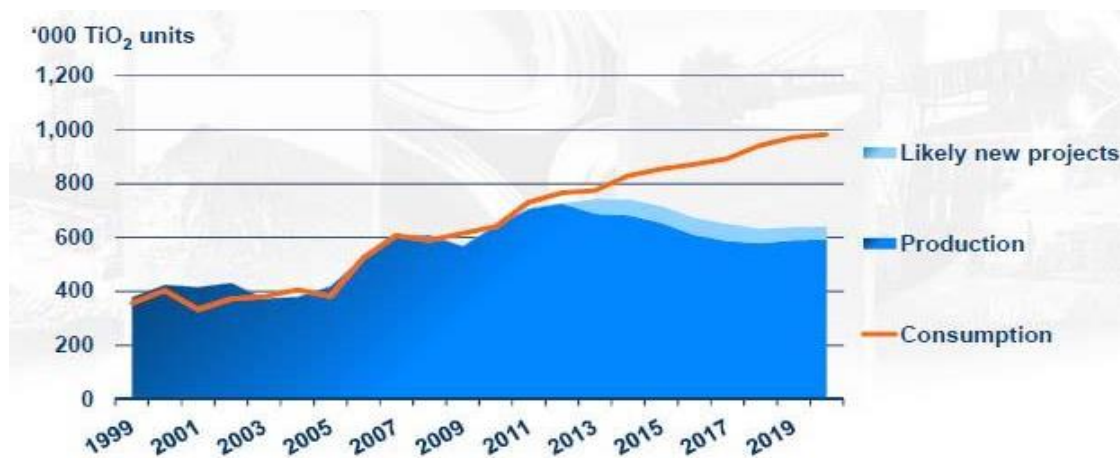
Figure 1-1: Rutile Supply/Demand, 1999-2020E (GMP, 2011).

Therefore, since heavy minerals are highly associated with ionizing radiation, a radiological hazard assessment and investigation of heavy minerals was carried out. Figure 1.2 and Figure 1.3 shows a cross section of the sampling sites with heavy minerals.

Figure 1-2: Heavy Mineral Sand in MwitaSyano River bed

Figure 1-3: A cross section of a sampling site showing presence of heavy minerals

1.1 Geology of Kitui area

The rocks in Kitui can be classified into four types: - Metamorphic rocks of the basement system, lacustrine sediments of the Mui valley, superficial deposits of recent age and tertiary dyke intrusions (Sanders, 1954). The basement system rocks in the area are gneisses, granulites, and schists including metamorphosed sediments. They have a roughly north – south trend.

According to Sanders (1954), the regionally metamorphosed rocks of undoubted sedimentary origin occur as crystalline limestones, graphitic gneisses, sillimanite gneisses, and quartzites. The lacustrine sediments of the Mui River Valley is a group of sands, clays, carbonaceous marcasite clays, thin shales and lignites of Pleistocene age, which have been proved to occupy a narrow sedimentary pocket in the valley of the Mui River up to a depth of 1,378 m (Sanders, 1954). Apart from the upper beds of the succession, which to a depth of 98.5 m or 131 m, consist of unconformable river sands and gravels, the sediments represent a deposit of argillaceous material showing a rhythmic variation in carbon content.

1.2 Problem Statement

The Mwita Syano River bed sands which possibly contain heavy minerals are mainly used for construction in Kitui County. However, these heavy mineral sands have the potential to contain high level of radionuclides. Therefore, this could lead to radiation exposure to the people who are involved in handling the heavy mineral sands. It was therefore, imperative to determine the potential radiological hazard in these sands. In addition, it was important that the heavy mineral present in the sands be investigated so as to reveal their economic potential, if any.

1.3 Objectives of the study
Overall objective
The main aim of this study was to investigate the heavy minerals of economic importance and also evaluate the potential of their radiological hazard in the Mwita Syano River bed sands.

Specific objectives

The specific objectives for this study were;

(i) To study the heavy minerals of economic importance present in Mwita Syano River bed sands.

(ii) To determine if there were any natural radioactivity radionuclides in the Mwita Syano River bed sands.

(iii) To evaluate whether the natural radioactivity posed any radiological hazards of the Mwita Syano River bed sands so as to advise the local community accordingly

Chapter 2

Literature Review

2.0 Introduction

Heavy mineral sands are formed from weathering of pre-existing rocks, and accumulated by wind or water (Farooq et al., 2010). This happens especially when the energy of the transport medium abates hence resulting in settlement of the heavy minerals (Elsner, 2010). Some of the heavy minerals contain uranium and thorium which are radioactive and hence they can be a potential source of gamma radiations which are harmful. Even though potentially harmful, these heavy minerals have numerous industrial applications and thus considered to be valuable. Therefore, this chapter will look at natural radioactivity and its health effects, and how it can be measured using gamma ray spectroscopy. Also, it will look into heavy mineral analysis and industrial applications of heavy minerals.

2.1 Natural radioactivity

Natural radioactivity is widespread in various environments on the surface of the earth such as earth crust, rocks, soils, plants, and water. There are two forms of radioactivity: those that come from the earth's crust (terrestrial radioactivity) and those which result from the interaction of atmospheric gases with cosmic rays (cosmogenic radioactivity). Terrestrial radioactivity in the earth's crust came into existence with the creation of the earth. Even though there are natural radioactive materials that have disappeared from the earth's surface, there are still some (NORM) which still exist and belongs to four radioactive decay series: uranium, thorium, actinium and neptunium. On the other hand, cosmogenic radioactivity comes from the collision of highly energetic cosmic ray particles with stable elements in the ground and atmosphere. The entire atmosphere, geosphere and all parts of the earth that directly exchange material with the atmosphere contain cosmogenic radionuclides. The major production of cosmogenic radionuclides results from the interaction of cosmic rays with atmospheric gases.

Uranium series

The parent radionuclide in this series is ^{238}U (abundance = 99.28 %) which undergoes α decay with half-life of about $4.47 * 10^9$ years. The stable product in this series is ^{206}Pb and is reached after 8α and 6β decays. Actually, the major form of natural radiation in this series is radon gas (^{222}Rn, Figure 2.1).
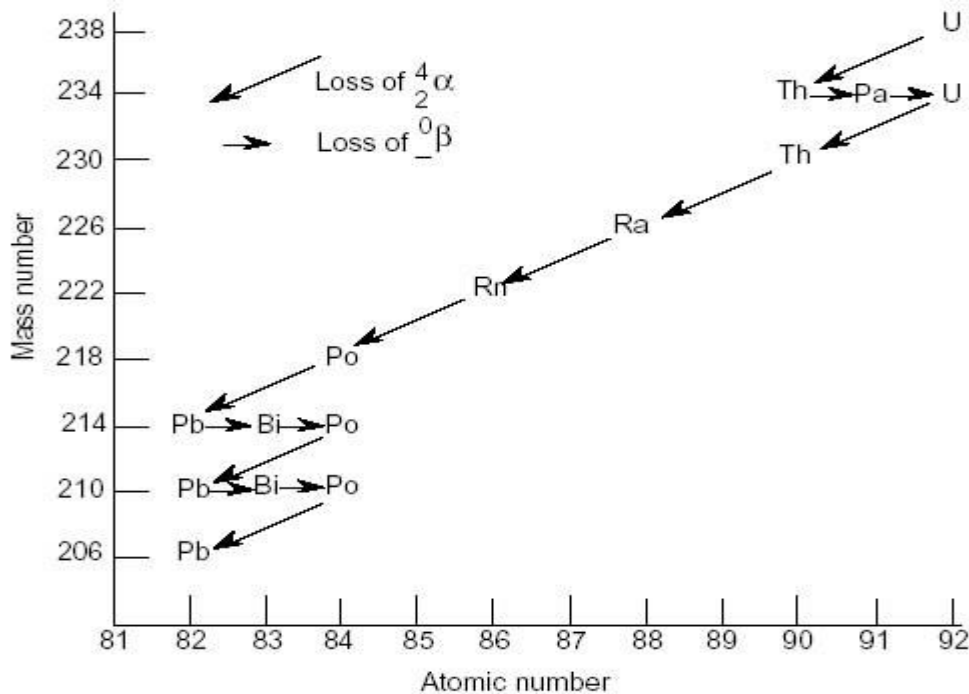
Figure 2-1: Uranium decay series (Adapted from Chang, 2005)

Radon gas is a natural occurring radionuclide and is commonly found in soils and rocks. It is a tasteless and colourless gas and is not reactive and therefore can accumulate up to dangerous levels without those living around that area realising that they are being exposed to radiation. It enters underground water and the air we breathe as it escapes from the ground. If the level of gas present is high, as in the case of a dwelling place with inadequate ventilation, it may cause cancer, lung cancer in particular. Radon gas contains decay products that are deposited in the lungs when it is inhaled. The ionizing radiation emitted by this product penetrates pulmonary tissues, bronchi, and mucous membrane cells. The action of radiation on bronchial cells is believed to set in motion the act of carcinogenesis. Usually, it is the upper airways which are affected by lung cancer, but radon gas gives rise to all types of tissue related lung cancers such as squamous cell

carcinoma, small cell carcinoma and adenocarcinoma.

Thorium series

The series begin with ^{232}Th radionuclide and has 100 % abundance and it undergoes decay with half-life of $1.41*10^9$ years. The series ends with a stable nuclide ^{208}Pb and is reached after 6α and 5β decays.
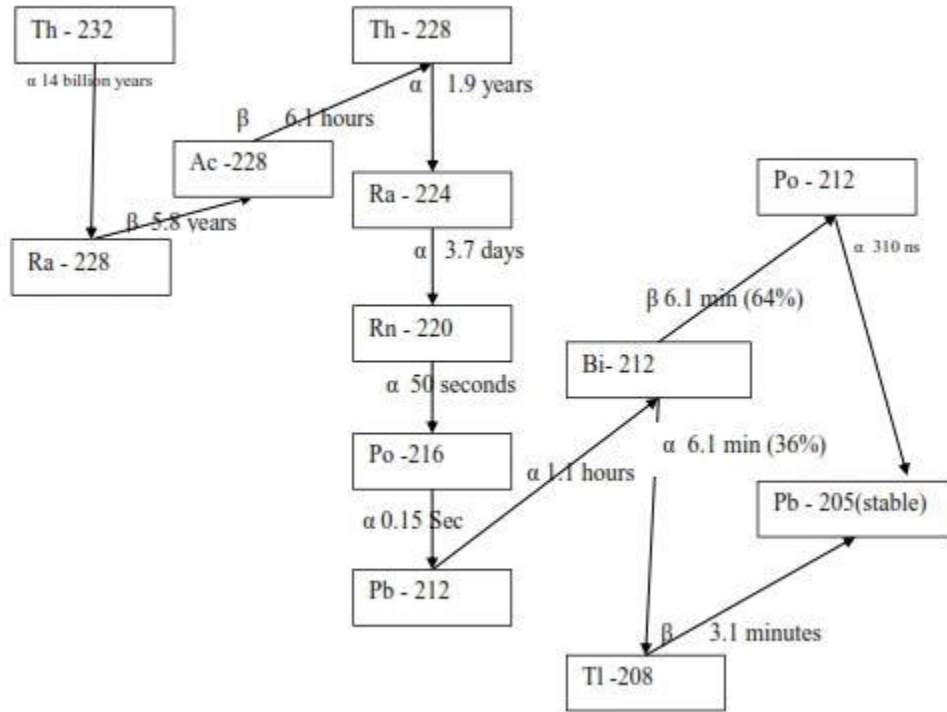
Figure 2-2: Thorium Decay series (ANL, 2005).

Actinium series:

It begins with ^{235}U which is the long lived nuclide in the series and it ends up with a stable isotope of ^{207}Pb. ^{235}U is an alpha-emitter with a complex alpha spectrum and a correspondingly complex gamma spectrum. The immediate decay product of ^{235}U is ^{231}Th which has a half-life of
26.64 h.

Neptunium series:

The series has been named after its longest lived nuclide ^{237}Np which is also the parent species with a half-life of $2.14*10^6$ years. The end product of the neptunium series is

8

^{209}Bi, which is the only stable isotope of bismuth. From ^{237}Np to ^{209}Bi 7α and ß decays are emitted.

Potassium (^{40}K)

^{40}K is another major source of terrestrial radioactivity. The long half-life of ^{40}K ($1.25*10^9$ years) means that it still exists in measurable quantities today. It decays mostly through β-emission to ^{40}Ca, and forms 0.012% of natural potassium. It is found in many foodstuffs and indeed fills an important dietary requirement, once taken in, potassium-40 behaves in the body in the same manner as other potassium isotopes. Humans require potassium to sustain biological processes, with most (including potassium-40) being almost completely absorbed upon ingestion, moving quickly from the gastrointestinal tract to the bloodstream. The potassium-40 that enters the bloodstream after ingestion or inhalation is quickly distributed to all organs and tissues. Then through the emitted ionizing radiation it can cause cancer.

2.2 The effects of radiation on health

Radiation damage to tissue and organs depends on the absorbed dose, the type of radiation and the sensitivity of different tissues and organs. The harmful health hazards of ionizing radiation on body tissues have been known for about 100 years. According to European Commission (2012), most of this knowledge was acquired by studying the survivors of the 1945 Japan atomic bomb attack. The research showed that high doses of radiation above 100 mSv can cause cancer, solid tumors and leukemia. In addition, it also has non-cancer effects, such as disrupting the structures and organic molecules that make up the cell. For example, deoxyribonucleic acid (DNA) which controls reproductive cells and all other cell activity. As a result these cells may be passed to the offspring and hence may lead to heritable diseases. For example, EC (2012) reports that an exposure of 100 mSv to a pregnancy between 8-15 weeks may lead to fetuses' brain damage.

Stochastic Health Effects

Stochastic effects are associated with long-term, low-level (chronic) exposure to radiation. Increased levels of exposure make these health effects more likely to occur, but do not influence the type or severity of the effect (EPA, 2012). Cancer is considered by

most people the primary health effect from radiation exposure. Simply put, cancer is the uncontrolled growth of cells. Ordinarily, natural processes control the rate at which cells grow and replace themselves. They also control the body's processes for repairing or replacing damaged tissue. Damage occurring at the cellular or molecular level, can disrupt the control processes, permitting the uncontrolled growth of cells cancer. This is why ionizing radiation's ability to break chemical bonds in atoms and molecules makes it such a potent carcinogen (EPA, 2012).

Other stochastic effects also occur. For example, changes in DNA can also be referred to as mutations. Sometimes the body fails to repair these mutations or even creates mutations during repair. The mutations can be teratogenic or genetic. Teratogenic mutations are caused by exposure of the fetus in the uterus and affect only the individual who was exposed. Genetic mutations are passed on to offspring.

Non-Stochastic Health Effects

Non-stochastic effects appear in cases of exposure to high levels of radiation, and become more severe as the exposure increases. Many non-cancerous health effects of radiation are non- stochastic. Unlike cancer, health effects from 'acute' exposure to radiation usually appear quickly. Acute health effects include burns and radiation sickness, which is also called 'radiation poisoning'. It can cause premature aging or even death. If the dose is fatal, death usually occurs within two months. The symptoms of radiation sickness include: nausea, weakness, hair loss, skin burns and diminished organ function (EPA, 2012).

2.3 Heavy Minerals

Several studies on various aspects of heavy minerals have been reported (Cook, 1969; Abuodha, 2003; Joshua and Oyebanjo, 2009; Choundry et al., 2010; Farooq et al., 2010; Oyebanjo et al. 2012). For example, Abuodha (2003), carried a study on grain size distribution and composition of modern dune and beach sediments in Malindi bay coast and found out that the average heavy mineral content of the sands were averaging 15 % by weight, with the highest concentration being 67 % by weight for the samples. Joshua and Oyebanjo (2009) on their part, carried out a study on the distribution of heavy

minerals in Osun River and found out that the most abundant heavy minerals was staurolite and rutile, which were 43.92 % and 11.95 % respectively of the heavy minerals. In the same study the combined zircon, tourmaline, and rutile percentage values were found to vary between 21.1% and 56.7%. In Pakistan, Choundry et al. (2010) showed that the Sonmiani, Boundniari and Phore sea beaches had 19.65 % ilmenite, 9.78 % altered ilmenite, 2.21 % of zircon, 1.93 % rutile, 0.21 % magnetite, 0.27 % leucoxene, 0.12 % garnet and 0.11 % of monazite. In that study, they concluded that the high percentages of the valuable minerals such as ilmenite and monazite were an indication that the minerals could be exploited for commercial purposes. Farooq et al., (2010) on their part reported that the percentage weights of ilmenite and monazite were found to be 19.6 % and 0.11 % respectively. The Table 2.1 shows some of the chemical composition and specific gravity of some of the heavy minerals.

Despite the fact that there are numerous heavy minerals only a few have economic significance due to their properties and prevalence (Elsner, 2010). These are called valuable heavy minerals and they include ilmenite, rutile, zircon, monazite, sillimanite, and garnet (Farooq et al., 2010) and also leucoxene, xenotime, staurolite, aluminum silica minerals, i.e.kyanite and andalusite, magnetite, chromite, cassiterite, tantalite-columbite, wolframite and scheelite (Elsner, 2010).

2.3.1 Heavy minerals of economic importance

Out of the numerous heavy minerals available, there are some of them which are economically important because of the compounds they contain. For example, ilmenite, leucoxene and rutile all have TiO_2 which has a number of industrial applications. Also, zircon ($ZrSiO_{4)}$ is considered a valuable mineral because it has numerous applications in the industries. This section therefore will focus on some of the heavy minerals which are economically important and also industrial applications.

Ilmenite, leucoxene and rutile and their industrial uses

Ilmenite, leucoxene, and rutile are all important ore minerals and they contain titanium dioxide (TiO_2) in progressively increasing amounts (Lener, 1997). TiO_2 is easily the most significant white pigment in the world, and is used, amongst other things, in paints and

varnishes, printing inks, plastics, rubber, linoleum, artificial fibres, paper, glass, enamel, and ceramics (Elsner, 2010). Generally about 95% of all titanium-bearing mineral such as rutile, ilmenite and leucoxene are used in the titanium dioxide pigment industry (Harben & Kužvart, 1996).

Table 2-1: Specific gravity of selected heavy mineral sands (Lener, 1997)

Mineral	Composition	Specific Gravity
Monazite	$(Ce,La,Y,Th)PO_4$	4.6 - 5.4
Magnetite	Fe_3O_4	5.18
Ilmenite	$FeO.TiO_3$	4.7
Zircon	$ZrSiO_4$	4.68
Chromite	$FeCr_2O_4$	4.6
Rutile	TiO_2	4.18 - 4.25
Spinel	$MgAl_2O_4$	3.5 - 4.1
Corundum	Al_2O_3	4.02
Anatase	TiO_2	3.9
Staurolite	$Fe_2Al_9O_6(SiO_4)_4(O,OH)_2$	3.65 - 3.75
Kyanite	Al_2SiO_5	3.55 - 3.66
Sphene	$CaO.TiO_2.SiO_2$	3.40 - 3.55

Ilmenite is the most common titanium mineral in the Earth's crust. It is mostly dispersed as accessory mineral in almost all intrusive and extrusive rocks (Elsner, 2010), where it is often associated with hematite or magnetite (Lener, 1997). All the three minerals mined as ore bodies in crystalline rocks or as secondary deposits in sand beaches and rivers (Cook, 1969).

Zircon and its industrial uses

Zircon ($ZrSiO_4$) is a non-magnetic and non-conducting heavy mineral which has a density of 4.68 g/cm^3. It compromises of ZrO_2 and SiO_2 by mass which forms 67.22 % and 32.78 % respectively (Elsner, 2010). In addition to the element zirconium (Zr), uranium (U), thorium (Th) and hafnium (Hf) which has the same chemical property as

zirconium are always found within zircon (Elsner, 2010). This renders zircon one of the main sources of radioactivity (Elsner, 2010). It is rarely found in minable concentration in rocks but due to its high specific gravity and resistance to weathering it can occur in minable concentrations in the "heavy mineral sands" of rivers, beaches and dunes (Cook, 1969). It is also often mined as a by-product from titanium minerals sands such as ilmenite and rutile Lener, 1997). About half the world's zircon production is used in the ceramic industry to provide opacity and whiten the ceramic materials (Harben, 1999). This is because of its high refractive index which enables opacification of melts and the white colouring of ceramic bodies (Elsner, 2010).

Monazite and Xenotime, and their industrial applications

The heavy minerals monazite and xenotime are members of the rare earths minerals (Elsner, 2010). Monazite minerals are composed of cerium, lanthanum, neodymium, thorium and phosphates {(Ce, La, Nd, Th) [PO] 4} while xenotime is made up of Y (PO4). Both the elements are paramagnetic and non-conducting. In addition, they can incorporate different quantities of uranium and especially thorium into their crystal lattices, and therefore can be a source of radioactivity (Elsner, 2010). Monazite is a major source of thorium and rare earth elements (lanthanum, cerium and neodymium) while xenotime contains yttrium, also a rare earth element (Elsner, 2010). Thorium is used as a fuel in some breeder reactors and in the manufacture of welding rods, refractory, etc. while the rare earths have numerous applications in the manufacture of catalysts used in petroleum refining and high-strength permanent magnets (NSW, 2007).

2.4 Radioactivity measurements

There are various techniques for example, liquid scintillation, Geiger Muller detector used to determine natural occurring radioactive materials (NORM) in geological, biological, and environmental media. However, one of the most powerful techniques that is commonly employed is the gamma ray spectroscopy.

Gamma Ray Spectroscopy

Radioactive materials produce gamma rays of various energies and intensities which can be used to detect the gamma source through gamma ray spectroscopy. An example of

instrument which employs gamma ray spectroscopy and is frequently used for identification and assessment of low radioactivity levels in different samples emitting gamma rays is the High Purity Germanium detectors (HPGe).

Assessment of radioactivity levels using HPGe

In order to use HPGe effectively, it has to be calibrated. There are two types of calibration which have to be done; energy calibration and photo peak detection efficiency calibration. Energy calibration is necessary to identify different isotopes from respective gamma ray energy lines while photo peak detection efficiency determination is necessary for quantitative assessment of the radioactivity levels for each radioisotope.

Energy Calibration

Energy calibration is the assigning of the correct energy value to the corresponding channel number. The pulse height is assumed to be proportional to the energy of the incident particle. In gamma-ray spectroscopy with germanium detectors, the pulse height scale must be calibrated in terms of absolute gamma-ray energy if various peaks in the spectrum are to be properly identified. In many applications, the gamma-rays expected to appear in the spectrum are well known in advance and the corresponding peaks can be identified by inspection. In other applications, unknown gamma-ray spectra may occur and hence a spectra calibration gamma ray source is used to identify the peaks of the unknown sample. Accurate calibration should involve a standard source with gamma-ray energies that are not widely different from those to be measured in the unknown spectrum and the selection of the standard depends on the energy range of interest.

Detection efficiency

Radiation such as gamma ray must first undergo a considerable interaction in the detector crystal before detection is possible and therefore their detectors are always not 100 % efficient. As a result, it is necessary to accurately identify all the pulses which have been detected.

2.5 Heavy Mineral Analysis

In order to determine the heavy minerals present in the black sands, X-ray Powder Diffraction (XRD) is commonly used. This is a technique that is usually used to study

crystalline materials. The three-dimensional structure of non-amorphous materials is defined by regular, repeating planes of atoms that form a crystal lattice. When a focused X-ray beam interacts with these planes of atoms, part of the beam is transmitted, part is absorbed by the sample, part is refracted and scattered, and part is diffracted. When an X-ray beam hits a sample and is diffracted, we can measure the distances between the planes of the atoms that constitute the sample by applying Bragg's Law. From Bragg's Law (equation 1), the characteristic set of d-spacing and their intensity generated in a typical X-ray scan provides a unique "fingerprint" of the phases present in the sample.

$$n\lambda = 2d\sin\theta, \tag{1}$$

where the integer n is the order of the diffracted beam, λ is the wavelength of the incident X-ray beam, d is the distance between adjacent planes of atoms (the d-spacing), and θ is the angle of incidence of the X-ray beam. Since we know λ and we can measure θ we can calculate the d- spacing.

Chapter 3

Research Methodology

3.0 Introduction

In this chapter, the geographical setting of the study area, sample preparation of heavy mineral sand and the method used for procedures are presented. Elemental quantification, heavy mineral quantification and radioactivity measurements are presented.

3.1 Area of study

The study area is Mwita Syano River, which is a seasonal river (figure 3-1). It is located in Kwa Vonza town, Kitui County, which is 140 km south east of Nairobi. It lies on the boundary of Machakos and Kitui County. It is easily accessible and during dry seasons it dries up completely. It has several tributaries such as Mikuyuni and Ikalumbatuni.
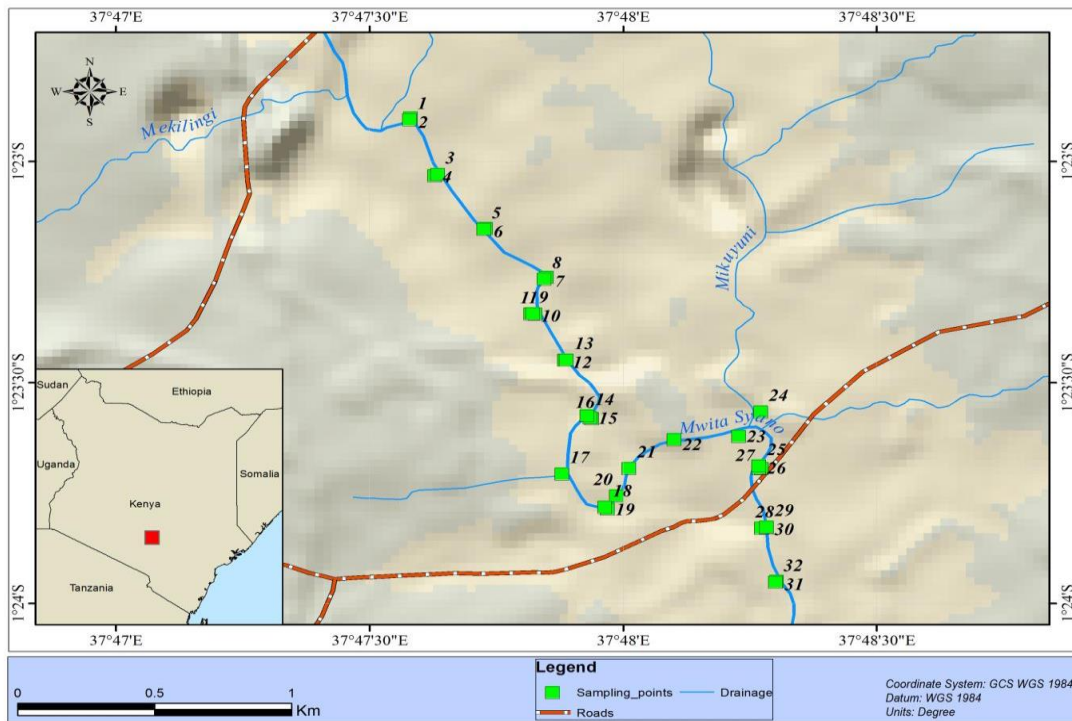

Figure 3-1: **Map of Mwita Syano River showing the location of the study area and the sampling points.**

3.2 Sample collection

A total of 41 representative sand samples were collected within a distance of 3 km on the river bed, 26 of which were collected within a depth of 0-20 cm and the remaining 15 were collected within a depth of 20- 50 cm. The samples were then put in plastic bags, labelled and transported to INST laboratory for measurements

Sample Preparation for radioactivity measurements

The .samples were sieved to grain size < 1mm. They were then put in a 250 cm^3 plastic containers for at least one month before counting to bring down radon (^{222}Rn) to its short lived progeny into equilibrium with ^{238}U, as per the standard set by IAEA (ASTM, 1986).

Sample preparation for XRD measurements

About 3 grams of the sample was put in the milling cup and then the equivalent of nine (9) grams of ethanol were added to have a weight of 12 grams. The cup was then capped and milled for about 12 minutes. The milled sample was then transferred into a 50ml centrifuge tube. The centrifuge was then set at 4000 rpm and then it was let to run for about 10 minutes to separate the supernatant liquid. Finally, hexane was added in the ratio of 0.5 ml to 1 g of the sample and the sample was dried between 85 ^{o}C to 105 ^{o}C for about one hour. The dried sample was then sieved through 250 μm sieve then poured into a glass vial and capped.

3.2 Radioactivity measurements

The samples were analysed for activity concentration using a high purity germanium (HPGe) spectrometer using three reference materials; RG-set (RG-U, RG-Th and RG-K). The HPGE spectrometer consisted of a HPGE detector, coupled to a personal computer based multi-channel analyser (MCA) along with spectroscopy amplifier and associated electronics. The detector is a dipstick geometry and cooled by liquid nitrogen.

3.3 Activity concentration measurements

Activity concentration of ^{226}Ra, ^{232}Th and ^{40}K were determined using the HPGE spectrometer. The analysis of ^{226}Ra was carried on the basis of the average of the gamma peaks of their daughter products (^{214}Pb and ^{214}Bi) while ^{232} Th measurement

was based on ^{228}Ac and ^{212}Pb which are its daughter products. Finally, the analysis of ^{40}K was based on its single peak of 1460 Kev.

The activity concentrations were determine using equation 2:

$$\frac{M_s \ X \ A_s}{I_s} = \frac{M_{ref} \ X \ A_{ref}}{I_{ref}} \tag{2}$$

where M_s = mass of the sample, A_s = activity of the sample, I_s = Intensity of the sample, M_{ref} = Mass of the reference sample, A_{ref} = Activity of the reference, and I_{ref} = Intensity of the reference sample.

3.4 Assessment of radiological hazards

Most of the Mwita Syano River bed sands are used for construction (figure 3.2). As such, the radiological hazards due to γ-ray radiation in these sands was determined using three different indices; radium equivalent (Ra_{eq}), Gamma index (I_{yr}) and finally external hazard index (H_{ex}).

In the calculation of the radiological hazards a secular equilibrium between ^{238}U and ^{226}Ra was assumed. This is due to the fact that about 98% of the external dose of ^{238}U is delivered by ^{226}Ra and therefore in case there is any disequilibrium between the two radionuclides it must be negligible (UNSCEAR, 2012).

Figure 3-2: Workers collecting sand for construction

3.4.1 Radium equivalent (Ra$_{eq}$) is a single term that represents the combined specific activities of [226] Ra, [232]Th and [238]U and is used to indicate the external dose to the public. This index is based on the fact that 370 Bq kg^{-1} of [226] Ra, 259 Bq kg^{-1}of [232]Th and 4810 Bq kg^{-1}of [40]K produce the same gamma ray dose rate. Therefore, the minimum Ra$_{eq}$ has to be less than 370 Bq kg^{-1} in order to keep the external dose to be less than 1.5 m Gy y^{-1}(UNSCEAR, 2010). The radium equivalent were determined using equation 3.

$$Ra_{eq} = A_{Ra} + 1.43A_{Th} + 0.077A_K \qquad\qquad (3)$$

where A_{Ra}, A_{Th} and A_K are the specific activities of [226]Ra, [232]Th and [40]K in Bq Kg^{-1} respectively. Another radiation hazard index is the representative **level index (I$_{yr}$) that** has been used by many researchers to assess the radiological hazards in building materials (EC, 1999). According to European Commission, EC (197 9), the I$_{yr}$ index should not be more than 1 Bq kg^{-1} which corresponds to annual

19

effective dose of 1 mSv yr^{-1}. The level index was calculated using the equation 4.

$$I_{yr} = (1/150)A_{Ra} + (1/100)A_{Th} + (1/1,500)A_{K}, \qquad (4)$$

where A_{Ra}, A_{Th} and A_{K} are the specific activities of ^{226}Ra, ^{232}Th and ^{40}K in Bq/Kg respectively.

The three radionuclides; ^{226}Ra, ^{232}Th and ^{40}K, upon decay produce gamma/ beta radiations which penetrate the air hence exposing making human beings to the harmful effects of ionising radiation. The main factors determining human being exposure rate are the concentrations of these radionuclides in a material and the time spent in the radiation area.

The radiation exposure in the outdoor to gamma rays is called the **hazard index (H$_{ex}$) and** is a radiation hazard index defined by EC (1979) as shown in **equation 5.** This index value must be less than unity to keep the radiation hazard insignificant, i.e. the radiation exposure due to the radioactivity from construction materials should be limited to 1.0 m Sv y^{1}.

$$H_{ex} = (A_{Ra}/370) + (A_{Th}/259) + (A_{K}/4810) \leq 1, \qquad (5)$$

where A_{Ra}, A_{Th} and A_{K} are the specific activities of ^{226}Ra, ^{232}Th and ^{40}K in Bq kg^{-1} respectively. The maximum value of H$_{ex}$ equal to unity corresponds to the upper limit of Ra$_{eq}$ (370 Bq kg^{-1}).

3.4.2 Dose rate calculation

The total air absorbed dose rate (nGy h^{-1}) at 1 m above the ground due to the specific activities of ^{226}Ra, ^{232}Th and ^{40}K (Bq kg^{-1}) was calculated using the equation 6 (UNSCEAR, 2000).

$$D^{\cdot} = 0.0417A_{K} + 0.462A_{Ra} + 0.604A_{Th} \qquad (6)$$

where $D^{\cdot}$ is the absorbed dose rate, A_{K}, A_{Ra} and A_{Th} are the activity concentrations for ^{40}K, ^{226}Ra and ^{232}Th respectively.

To estimate the annual effective dose rates, the conversion coefficient from absorbed

dose in air to effective dose (0.7 Sv gy^{-1}) and outdoor occupancy factor (0.2) proposed by EC, (1979) was used. The effective dose rate in units of mSv yr^{-1} was calculated by equation 7:

$$H_E = D \cdot TF, \tag{7}$$

where $D\cdot$ is the calculated dose rate (in nGy h^{-1}), T is the outdoor occupancy time (24 h x365.25 days x 0.2 = 1,753 h yr^{-1}), and F is the conversion factor (0.7 Sv gy^{-1}).

Chapter 4

Results and Discussions

4.0 Introduction

In this chapter, the experimental results of the research will be presented. The specific activity concentration and radiological hazards indices of the samples will also be compared to the literature values. In addition, they will also be compared to the limits set by UNSCEAR, ICRP and OECD in order to find out if the sands are radiologically safe. Finally, the XRD results will also be presented and discussed. In particular the results will be evaluated to determine if the sands contain heavy minerals of economic importance and their significance.

4.01 Quality Assurance

In determining the activity concentration of the samples, three reference materials were used as per IAEA recommendations (ASTM, 1986). These reference materials were RG-U, RG-Th and RG-K as shown in tables 4.1, 4.2 and 4.3 respectively.

Table 4-1: Activities of RG-U (Bq kg^{-1})

Analyte	Value	Unit	95% C.I.	N	R/I/C
^{235}U	228	Bq kg^{-1}	226 - 230	None	R
^{238}U	4940	Bq kg^{-1}	4910 - 4970	None	R
^{40}K	<0.63	Bq kg^{-1}	-	None	I
K	<20	mg kg^{-1}	-	None	I
Th	<1	mg kg^{-1}	-	None	R
U	400	mg kg^{-1}	398 - 402	None	R

Table 4-2: Activities of RG-Th (Bq kg^{-1})

Analyte	Value	Unit	95% C.I.	N	R/I/C
^{232}Th	3250	Bq kg^{-1}	3160 - 3340	155	R
^{235}U	3.6	Bq kg^{-1}	3.3 - 3.9	145	R
^{238}U	78	Bq kg^{-1}	72 - 84	145	R
^{40}K	6.3	Bq kg^{-1}	3.1 - 9.5	45	I
K	200	mg kg^{-1}	100 - 300	45	I
Th	800	mg kg^{-1}	784 - 816	155	R
U	6.3	mg kg^{-1}	5.9 - 6.7	145	R

Table 4-3: Activities of RG-K (Bq kg^{-1})

Analyte	Value	Unit	95% C.I.	N	R/I/C
^{40}K	14000?	Bq kg^{-1}	13600 - 14400	20	R
K	448000	mg kg^{-1}	445000 - 451000	20	R
Th	< 0.01	mg kg^{-1}	-	20	I
U	< 0.001	mg kg^{-1}	-	20	I

4.1 Gamma Spectroscopy Results

The specific average activities of ^{212}Th, ^{226}Ra and ^{40}K for the samples collected between 0-20 cm were found to be 12.4 Bq kg^{-1}, 7.4 Bq kg^{-1} and 317 Bq kg^{-1} respectively (Table 4.4).

Table 4-4: Average specific activity concentration (Bq kg^{-1}) of the samples collected between 0-20 cm

S.No	^{232}Th	^{226}Ra	^{40}K
1	7.1 ± 1.4	4.8 ± 0.5	111 ± 69
2	23.6 ± 1.6	12.0 ± 1.1	367 ± 12
3	12.4 ± 1.4	7.2 ± 1.1	379 ± 12
4	25.3 ± 1.6	9.1 ± 1.1	381 ± 11
5	5.0 ±1.0	4.8 ± 1.3	322 ± 14
6	13.6 ± 2.4	7.0 ± 1.0	339± 17
7	6.6 ± 0.8	2.8 ± 0.5	303 ± 9
8	7.8 ± 0.8	3.8 ± 0.4	310 ± 16
9	6.1 ± 0.6	7.7 ± 0.8	321 ± 12
10	3.1 ± 0.3	4.5 ± 0.5	390 ± 19
11	6.4 ± 1.3	5.9 ± 1.0	318 ± 10
12	19.2 ± 2.4	8.1 ± 0.8	425 ± 21
13	11.9 ± 1.4	7.4 ± 0.8	331 ± 13
14	5.2 ± 0.5	5.0 ± 0.5	299 ± 11
15	12.5 ± 1.2	6.4 ± 0.6	324 ± 32
16	8.3 ± 0.8	7.0 ± 0.7	315 ± 23
17	7.9± 0.8	12.4 ± 1.2	369 ± 22
18	25.1 ± 4.2	13.6 ± 2.7	220 ± 14
19	28.9 ± 2.9	12.0 ± 1.2	194 ± 2
Mean	12±1.4	7.4 ±0.9	317±18

On the other hand, samples collected at a depth of 20-50 cm had an average specific activity of 16. 1 Bq kg^{-1} of ^{232}Th, 10.4 Bq kg^{-1} of ^{226}Ra and 344 Bq kg^{-1} of ^{40}K (Table 4.5).

Table 4-5: Activities of the samples collected at 20-50 cm

S.No	^{232}Th	^{238}U	^{40}K
27	21.5 ± 2.2	10.3 ± 1.0	391 ± 39
28	**47.3 ± 7.1**	**35.7 ± 5.2**	**459 ± 54**
29	17.2 ± 2.3	7.0 ± 0.7	335 ± 20
30	7.5 ± 1.5	6.6 ± 1.1	344 ± 12
31	5.3 ±0.9	4.5 ± 0.5	335 ± 12
32	5.0 ± 0.8	5.8 ± 0.3	254 ± 7
33	7.5 ± 0.8	6.3 ± 0.6	353 ± 21
34	17.3 ± 2.3	6.9 ± 1.2	277 ± 12
Mean	16.1 ± 2.2	10.4 ± 1.3	344 ± 2

From tables 4.4 and 4.5, it is evident that the specific activities of the samples collected at a depth of (20-50) cm have a higher mean of specific activities than those collected at a depth of (0-20) cm. For example, the samples collected at a depth of 0-20 cm has a ^{232}Th specific activity of 12.4 Bq kg^{-1}. This specific activity is lower than 16.1 Bq kg^{-1} for ^{232}Th which at a depth of 20-50 cm. This difference may be because of the fact that the heavy sands sink to the bottom. Therefore, the concentrations of the radionuclides are likely to be higher as the depth increases because of their higher densities than the other minerals which are light. It can also be noted that samples 27 and 28 have high specific activities as compared to the other sample. This may be attributed to the fact that it was collected in a deposition area and hence there are higher chances that majority of the heavy minerals were present at that particular point.

4.1.1 Activities of samples collected at the same point but at different depths

This section shows the activities of pairs of samples collected at the same point. The samples which were collected at a depth of 0-20 cm are named "a" while those collected at a depth of 20-50 cm are named "b". The activities of these samples are presented in table 4:6.

Table 4-6: Activities of the samples collected at a depth of 0-20 cm and 20-50 cm on the same sampling point

S No.	Depth (cm)	^{232}Th	^{238}U	^{40}K
20 a.	0-20	8.7 ± 1.2	6.9 ± 0.7	344 ± 11
20 b.	20- 50	6.4 ± 1.2	6.5 ± 0.6	344 ± 16
21a.	0-20	8.5 ± 1.9	6.8 ± 1.2	303 ± 17
21 b.	20- 50	12.4 ± 1.4	9.4 ± 0.9	271 ± 11
22 a.	0-20	7.3 ± 1.2	4.9 ± 0.8	270 ± 12
22 b.	20- 50	15.3 ± 1.9	8.0 ± 1.5	322 ± 16
23 a.	0-20	12.1 ± 1.6	7.4 ± 1.3	338 ± 14
23 b.	20- 50	28.0 ± 3.6	10.9 ± 1.1	223 ± 26
24 a.	0-20	16.4 ± 1.9	8.6 ± 1.4	446 ± 16
24 b.	20- 50	6.7 ± 1.1	5.9 ± 0.9	344 ± 11
25 a.	0-20	10.1 ± 1.5	8.9 ± 1.1	365 ± 46
25 b.	20- 50	14.7 ± 1.5	6.4 ± 1.1	361 ± 13
26 a	0-20	28.9 ± 3.4	12.0 ± 2.1	194 ± 21
26 b.	20-50	11.2 ± 1.1	5.5 ± 0.6	273 ± 12
Mean		13.3 ± 1.8	7.7 ± 1.1	314 ± 17

In general these samples have an average of 13.3 Bq kg^{-1} of ^{212}Th, 7.7 Bq kg^{-1} of ^{226}Ra and 314 Bq kg^{-1} of ^{40}K as shown in table 4.2. However, when these pairs of samples are compared, there is no clear conclusion that can be arrived at. For example, looking at sample 21a and 21 b, it is evident that 21b has a higher ^{232}Th concentration than 21a. However, in terms of ^{238}U then the opposite is true as can be seen in table 4.6.

In order to find out if the concentration of the radioactive elements at 0-20 cm has any correlation with those collected at a depth of 20-50 cm, a correlation analysis was carried out. The analysis showed that there was hardly any correlation for ^{232}Th radionuclide as shown in figure 4.1. This variation may be caused by the fact that these radionuclides are found in the river bed, therefore, there is a high chance that during rainy season the mineral composition of these sands are interfered with. Alternatively, may be the parent rocks from which the mineral was incorporated are light in terms of density, therefore they have been transported to other areas through wind and water erosion.
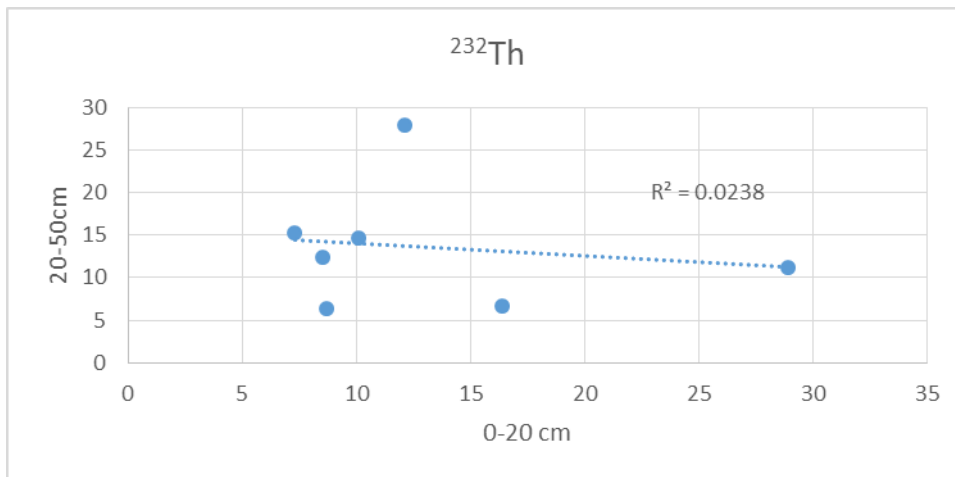
Figure 4-1: Regression analysis for ^{232}Th collected a depth of 0-20 cm and 20-50 cm

As for ^{238}U concentration a correlation coefficient of 0.55 ($r^2 = 0.3008$) (Figure 4.2) was found. This means that there is a close relationship between the ^{232}Th radionuclide found on the surface and those found at a depth of 20-50 cm.
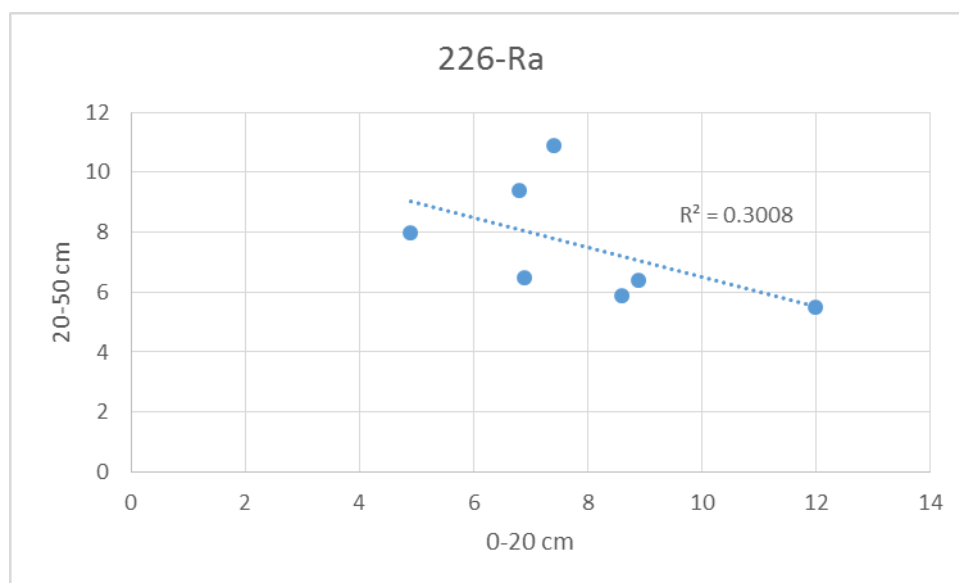

Figure 4-2: Regression analysis for ^{238}U collected a depth of 0-20 cm and 20-50 cm

However, a poor correlation was noted for ^{40}K (Figure 4.3). This may have been caused by the unpredictable water erosion which occurs on the river.
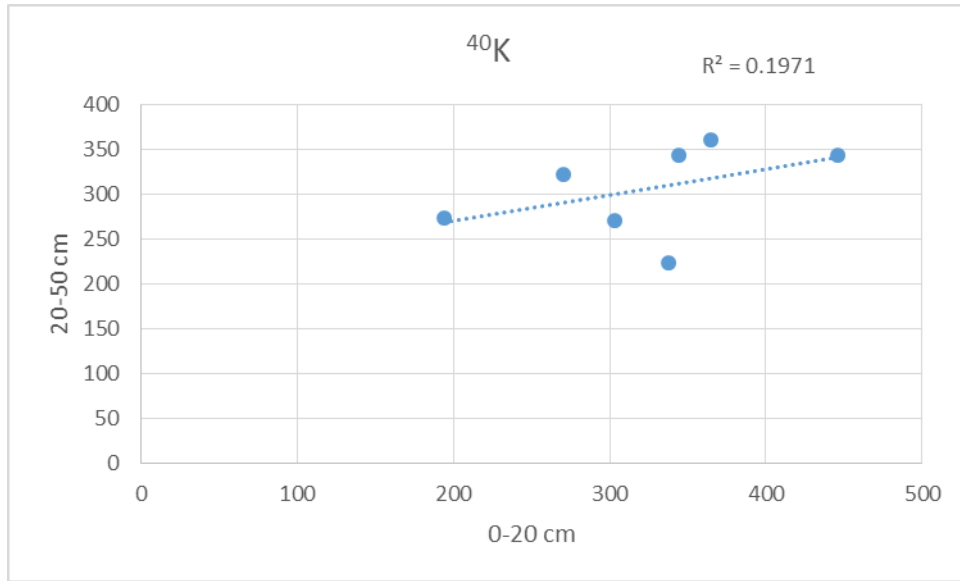
Figure 4-3: Regression analysis for ^{40}K collected a depth of 0-20 cm and 20-50 cm

4.1.2: The combined results

The activity concentration of ^{232}Th, ^{226}Ra and ^{40}K in the sand from Mwita Syano River bed vary as follows: 3.1 ± 0.3 Bq kg^{-1} to 47.3 ± 7.1 Bq kg^{-1} for ^{232}Th, 2.8 ± 0.5 Bq kg^{-1} to 35.7 ± 5.2 Bq kg^{-1} for ^{238}U , 110 ± 68.9 Bq kg^{-1} to 458 ± 54.2 Bq kg^{-1} for ^{40}K. The average specific activity for ^{232}Th, ^{226}Ra and ^{40}K on the other hand was 13.4 Bq kg^{-1}, 8.1 Bq kg^{-1} and 321 Bq kg^{-1} respectively. It is observed that the activity concentration of ^{40}K is much higher than ^{232}Th and ^{238}U, this may be attributed to the greater abundance of ^{40}K in the earth's crust. Also, this may be due to the presence of radioactive rich granites, sandstones and quartzite in the area as attributed to the geology of Kitui indicated by Sanders (1954). Compared to the results obtained by Malik (2013), the activity concentration obtained in Mwita Syano River bed lies within the range reported by the two authors along River Indus in Pakistan. For example, the two authors found that ^{226}Ra concentration varied between 4.82 Bq kg^{-1} and 155.50 Bq kg^{-1} for ^{226}Ra while the present study found that it ranges from 2.8 Bq kg^{-1} and 35.70 Bq kg^{-1} (Table 4.7).

Table 4-7: Average specific activity concentration (Bq Kg^{-1}) obtained in Kenya and River

Location	^{226}Ra	^{232}Th	^{40}K	References
River Indus	45.6	74.7	339.8	Malik, 2013
Sand used in Turkey	52	39	324	Cevik et al., 2009
Present Study	8.1	13.4	321	

4.1.2: Radiological hazard indices

The values for Ra_{eq}, I_{yr}, H_{ex}, D_{out}, and H_E were calculated using the activity concentration of ^{226}Ra, ^{232}Th and ^{40}K and the results are presented in table 4.8. The summary statistics showed that the radium equivalent (Ra_{eq}) are in the range of 23.4 – 139 Bq kg^{-1} and the average value is 52.1 Bq kg^{-1}. The average value of Ra (eq) is much less than the world average of 160 Bq kg^{-1} and certainly much smaller than the acceptable limit of 350 Bq kg^{-1}. The total air absorbed dose rate (Dose) 1 m above the ground has 11.1 nGy h^{-1} as the minimum value and 64.2 nGy h^{-1} as the maximum value. The average value of 25.3 nGy h^{-1} is much less than the world average of 58 nGy h^{-1}. The annual effective dose (AED) has a range of 0.014- 0.079 mSv and a mean of 0.031 mSv. The average value is less than the world average which is about 0.07 mSv yr^{-1}. The representative level index (I_{yr}) also had its values within the acceptable limit of 1Bq Kg^{-1}. All the values were lying between 0.176 – 1.02 Bq kg^{-1}. The average value 0.402 Bq kg^{-1} is within the acceptable limit of 1.0 Bq kg^{-1}. Even though sample nb1 still had high representative level index. In general all the samples were within the acceptable ranges of the radiological hazard limits. In general all the values were within the accepted range of (350 Bq kg^{-1} for Ra_{eq}, 1 Bq kg^{-1} for I_{yr}, and 10-200 for Dose) (OECD, 1979). Also, the annual effective dose was below 0.07 mSv yr^{-1} as recommended by the International Commission on Radiological Protection (ICRP, 1979) as the maximum annual dose for the public.

Table 4-8: Values of Dose, radium equivalent, annual effective dose, representative level index, and external hazard index

S.No	1	2	3	4	5	6	7	8	9	10	11	12	13
Radium Equiv.	23.4	74.0	54.2	74.7	36.8	52.6	35.6	38.9	41.3	39.0	39.6	68.3	49.8
Dose	11.1	35.1	26.6	35.4	18.7	25.6	17.9	19.4	20.7	20.2	19.9	33.1	24.4
Annual Effective Dose	0.014	0.043	0.033	0.043	0.023	0.031	0.022	0.024	0.025	0.025	0.024	0.041	0.030
Representative level	0.176	0.561	0.425	0.568	0.297	0.409	0.287	0.310	0.327	0.321	0.316	0.530	0.389

S.No	14	15	16	17	18	19	27	28	29	30	31	32	
Radium Equiv.	35.5	49.2	43.1	52.0	66.5	68.3	71.1	139.0	57.4	43.8	38.0	32.4	
Dose	18.0	24.0	21.4	25.9	30.6	31.1	34.0	64.2	27.6	21.9	19.3	16.2	
Annual Effective Dose	0.022	0.029	0.026	0.032	0.038	0.038	0.042	0.079	0.034	0.027	0.024	0.020	
Representative level	0.285	0.383	0.339	0.407	0.489	0.498	0.544	1.016	0.442	0.348	0.307	0.257	

S.No	33	34	20 a	20 b	21 a	21 b	22 a	22 b	23 a	23 b	24 a	24 b	25 a
Radium Equiv.	44.3	53.1	45.8	42.2	42.3	48.0	36.2	54.8	50.7	68.0	66.4	42.0	51.4
Dose	22.2	25.2	22.8	21.2	20.9	23.2	18.0	26.4	24.8	31.2	32.5	21.1	25.4
Annual Effective Dose	0.027	0.031	0.028	0.026	0.026	0.028	0.022	0.032	0.030	0.038	0.040	0.026	0.031
Representative level	0.353	0.404	0.362	0.337	0.333	0.368	0.286	0.422	0.395	0.501	0.519	0.336	0.403

4.2 XRD Results

The XRD analysis showed that the percentage concentration of albite ranges between 19.70 % to 27.20 % and its average percentage concentration is 23.46 %. On the other hand diopside percentage varied from 0% to 4.50% and its average percentage is 2.69%. In addition, it can also be noted that hornblende has percentage range of 8.10 % to 13.20 % while magnetite was found to vary from 0 % to 1.80 %. Finally orthoclase and quartz were found to range between 0% to 10.40% and 48.30% to 64.50 % (Table 4.9).

Table 4-9: Percentage of heavy mineral available in selected samples

Sample	Albite	Diopside	Hornblende	Magnetite	Orthoclase	Quartz
2	23.1	4.5	8.1	0	0	64.4
6	20.5	3.7	11.3	0	0	64.5
7	22.7	3.8	10.9	0	0	62.7
12	24	2.9	9.7	0	0	63.4
13	25.6	3.5	11.5	0	0	59.4
16	20.7	4	13.2	0	0	62.2
20a	19.7	0	8.4	0	10	61.9
22b	25.5	1.7	8.7	0	7.6	56.5
23a	**21.4**	**0**	**10.1**	**1.8**	**8.2**	**58.5**
27	25.1	2.5	9.1	0	10.4	52.8
28	26	2.6	9.1	0	9.6	52.7
29	27.2	3.1	11.8	0	9.6	48.3
Average	23.46	2.69	10.16	0.15	4.62	58.94
SD	2.37	1.40	1.51	0.50	4.67	5.09
Max.	27.20	4.50	13.20	1.80	10.40	64.50
Min.	19.70	0.00	8.10	0.00	0.00	48.30

The XRD analysis showed that several valuable minerals such as albite, diopside, hornblende, orthoclase and magnetite exist in these sands. Albite is an important ingredient in some building and ornamental stones, notably granites, some of the finest of which owe their beauty to feldspar crystals. For example, albite from the pegmatite veins of south-eastern Pennsylvania and north- eastern Maryland has been mined in

the past for use in pottery manufacture (NSW, 2007).

Orthoclase is also a valuable mineral and is used in making the body composition of several types of porcelain, earthenware and also in the preparation of glazes and enamel. In addition, it is used as an important ingredient in the glass sand batch and as a bonding agent in the manufacture of bonded abrasives like wheels and discs of garnet, corundum, emery, etc. The majority of the samples had a lot of quartz this may be because of the higher percentage of quartzite in Katui region (Sanders, 1954). The only available heavy mineral of economic importance in the selected samples is magnetite which was present in sample 23a and it formed about 1.8 % of the sample. Magnetite has a chemical formulae (Fe_3O_4) and is mainly used as an ore of iron, as an abrasive and an as a toner in the electrophotography.

The study revealed that the percentage albite present in the sands is about 23.46%, hornblende average is about 10.16% and orthoclase mean is 4.42%. These mineral percentages are quite high and therefore they may be economically viable. The current titanium dioxide being mined in Kwale County by Base Titanium Company forms about 4.4 % of the ore reserve (Base Titanium, 2015) and is being mined economically. Hence, the albite, orthoclase and hornblende can be mined for economical purposes.

The following figure 4.5 shows a spectrum section obtained after analysing sample 23a using XRD. The spectrum after being analysed using Eva software revealed that albite formed 25.1 %, diopside was about 2.5% and hornblende percentage was 9.1%. Also, orthoclase and quartz formed about 10.5% and 52.8% respectively.
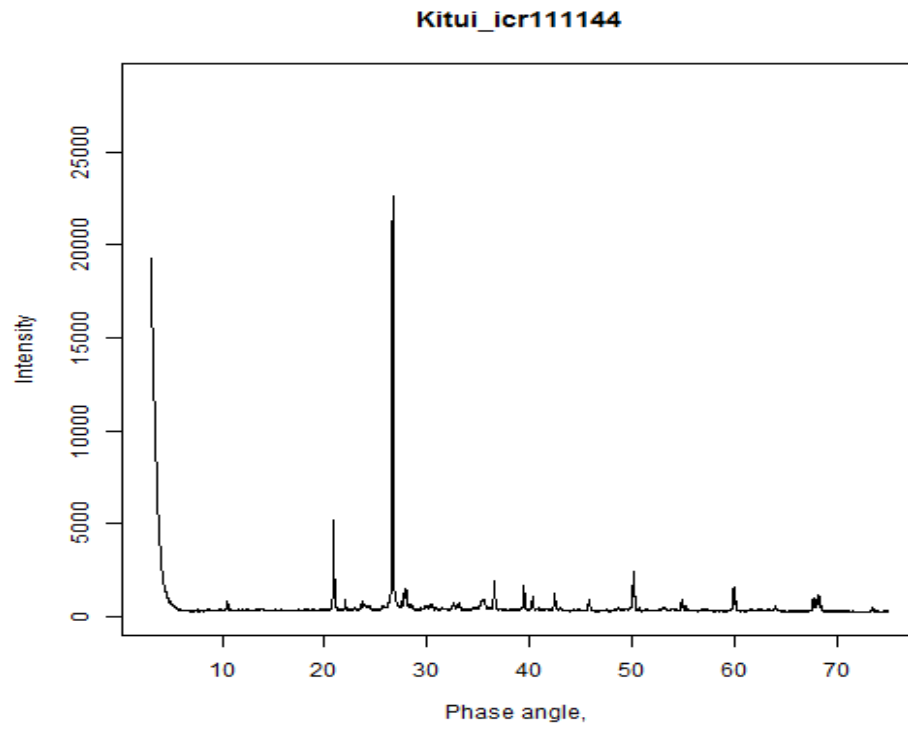
Figure 4-4: XRD spectrum for sample 23a

Chapter 5

Conclusion and Recommendations

5.1 Conclusion

These results show that the Mwita Syano River bed sands are not radiologically harmful because the average specific activity values were below the world average values. The result also showed that the only heavy mineral of economic importance available on the Mwita Syano River bed sands is magnetite which was found in sample (23a) and had a percentage of 1.8%. However, other minerals which are also valuable were found within the sands. These minerals were orthoclase which had an average percentage of 4.620% and albite which had an average percentage of 23.46% .

5.2 Recommendations

More research should be carried out on Mwita Syano River bed sands because the sampling for this study was done only up to a depth of 50 cm. This was because during the sampling period the sands were wet, and it was therefore was impossible to go beyond 50 cm. In addition, most of heavy minerals are dense therefore most likely they will settle at a lower depth as compared to the light minerals. The presence of magnetite in the samples which formed 1.8 % of sample 23a is enough evidence to show that there could be more heavy minerals in the sands. Since XRD analysis was done for only 12 samples we recommend a more elaborate study where many samples are analysed for their mineralogy using XRD. This will present a better picture on the presence or absence of minerals of economic viability.

References

Abuodha, J. O. Z. (2003). Grain size distribution and composition of modern dune and beach sediments, Malindi Bay coast, Kenya. *Journal of African Earth Sciences*, *36*(1), 41-54.

Alencar, A. S., & Freitas, A.C. (2004): Reference levels of natural radioactivity for the beach sands in a Brazilian south eastern coastal region. *Radiation measurement* (**40)**, pp. 76-83

Al-jundi, J. (2002). Population dose from terrestrial gamma exposure in areas near to Old phosphate mine, Russaifa, Jordan. *Radiation measurement* (**35)**, pp. 23-28.

Argonne National Laboratory, EVS. 2005. *Human Health fact Sheet: Asian Transactions on Basic and Applied Sciences,* 02 (04). ATBAS ISSN: 2221-4291.

ASTM. 1986. *Recommended practice for investigation and sampling soil and rocks for engineering purpose*. Annual Book of ASTM Standards (04.08). Report 420. ASTM, pp.109– 113

Base Titanium (2015). Project Overview. Retrieved from http://basetitanium.com/kwale-project/project-overview

Cevik, U., Damla, N., Kobya, A. I., Celik, N., Celik, A., & Van, A. A. (2009). Assessment of natural radioactivity of sand used in Turkey. *Journal of Radiological Protection*, *29*(1), 61.

Chang, R. (2005). Nuclear Chemistry. New York: MC-Grill.

Choppin, G. R., Rydberg, R., & Liljenzin, J. O. (1995). *Radiochemistry and Nuclear Chemistry,* 2 Ed. New York: Pergmon Press.

Choudry, M. A. F., Nurgis, Y., Hussain, A., & Abbasi, H. N. (2010). Distribution and Percentage of Heavy Minerals along Makran Coastline of Pakistan.

Cook, D. J. (1969): heavy minerals in Alaskan beach sand deposits. *Mineral Industry Research Laboratory University of Alaska College* 20, pp. 4-5.

Elsner, H. 2010. *Heavy Minerals of Economic Importance*. Hannover: Autumn.

Emsly, J. (1992).*The Elements*, 2 Ed. Oxford: Oxford University press.

European Commission (2012). *Understanding the effects of radiation on health.* Retrieved from http://ec.europa.eu/research/energy/pdf/radhealth_1.pdf

Farooq, M. A., Choudry, Y. N., Asif, H., & Abbasi, H. N. 2010. Distribution and Percentage of Heavy Minerals along Makran Coastline of Pakistan. *American Journal of Scientific Research* 11, pp.86-91.

GMP Securities Europe LLP .2011. *African Mineral Sands*. New York: Wiley.

Harben, P.W. & Kužvart, M. 1996. Industrial minerals: a global geology. London: Industrial Minerals Information Ltd.

Harben, P.W. 1999. The industrial minerals handy book, 3rd Ed. London: Industrial Minerals Information Ltd.

Hashim, N. O., Rathore, I. V. S., Kinyua, A. M., & Mustapha, A. O. (2004). Natural and artificial radioactivity levels in sediments along the Kenyan coast. *Radiation physics and chemistry*, *71*(3), 805-806.

Ivanovich, M., & Harmon, R. S. (1992). *Uranium-series disequilibrium:* Application to earth marine and environmental sciences. Oxford: Clarendon Press.

In Bruce, D. W., In O'Hare, D., & In Walton, R. I. (2014). *Structure from diffraction methods*. New York: Wiley

Joshua, E. O. & Oyebanjo, O. A. 2009. Distribution of Heavy Minerals in Sediments of Osun River Basin South-Western Nigeria. *Research Journal of Earth Sciences* (1), pp.74-80. Knoll**,** G. F. 1979. *Radiation detection and measurements*. New York: John Willey and sons.

Lener, E. F. (1997). *Mineral chemistry of heavy minerals in the old hickory deposit, Sussex and Dinwiddie Counties, Virginia*. Virginia Polytechnic Institute and State University. Mineralogical characterization of Vellar river sediments. *Bull. Pure Appl. Sci.,* 25(1). Pp.49-55.

Malik, F. (2014). Natural radioactivity in sand samples collected along the bank of river Indus in the area spanning over Gilgit to Lowarian, Pakistan: assessment of its radiological hazards. *Journal of Radioanalytical and Nuclear Chemistry*, *299*(1), 373-379.

NSW department of primary industry. 2007. Industrial mineral opportunities in New South Wales. *Geoscience publications.* **33**.

Nuclear Energy Agency Organization for Economic Cooperation and Development (NEA-OECD). (1979). *Exposure to Radiation from Natural Radioactivity in Building Materials.* Report by the NEA Group of Experts, OECD, Paris.

Oyebanjo, O. A., Joshua, E.O., & Jibiri, N. N. (2012). Characterization of Non-Opaque Minerals and naturally occurring Radionuclides in Sediments of   Osun River, Southwestern Nigeria.

Pincock Perspective. (2005). *Mineral Sands.* **66**. New York: Wiley.

Ramasamy, V., P.Rajkumar and V. Ponnusamy. 2009. FTIR spectroscopic analysis and Mineralogical characterization of Vellar river sediments. *Bull. Pure Appl. Sci.,* 25(1): 49-55.

Sanders, L. D. (1954). Geology of the Kitui area. *Geology Survey of Kenya,* Report No. 30.

Sundararajan, M. K. H., Bhat, & Velusamy, S. 2010. Investigation on Mineralogical and Chemical Characterization of Ilmenite Deposits of Northern Kerala Coast, India.*Research Journal of Earth Sciences* 2 (2), pp. 36-40.

The International Commission on Radiological Protection, *ICRP* (1990). *Recommendations of the ICRP, Publication 60*. Pergamon Press. Oxford, UK.

United Nations Scientific Committee on the Effects of Atomic Radiation (UNSCEAR). 2012. *Sources and effects of ionizing radiation. Report to the General Assembly*,

Annexe B. US, Environmental Protection agency (EPA). 2013. *Radiation: Non-Ionizing and Ionizing.* Retrieved from: http://www.epa.gov/radiation/understand/

Veiga, R., Sanches, N., Anjos, R. M. et al. (2006). Measurement of natural radioactivity in Brazilian beach sands. *Radiation Measurements* 41, Pp.189–196.

Yablokov, A., V., Nesterenko, V. B., & Nesterenko, AV. 2009. Chernobyl Consequences of the Disaster for the Population and the Environment. *Science journal.* Pp. 1189
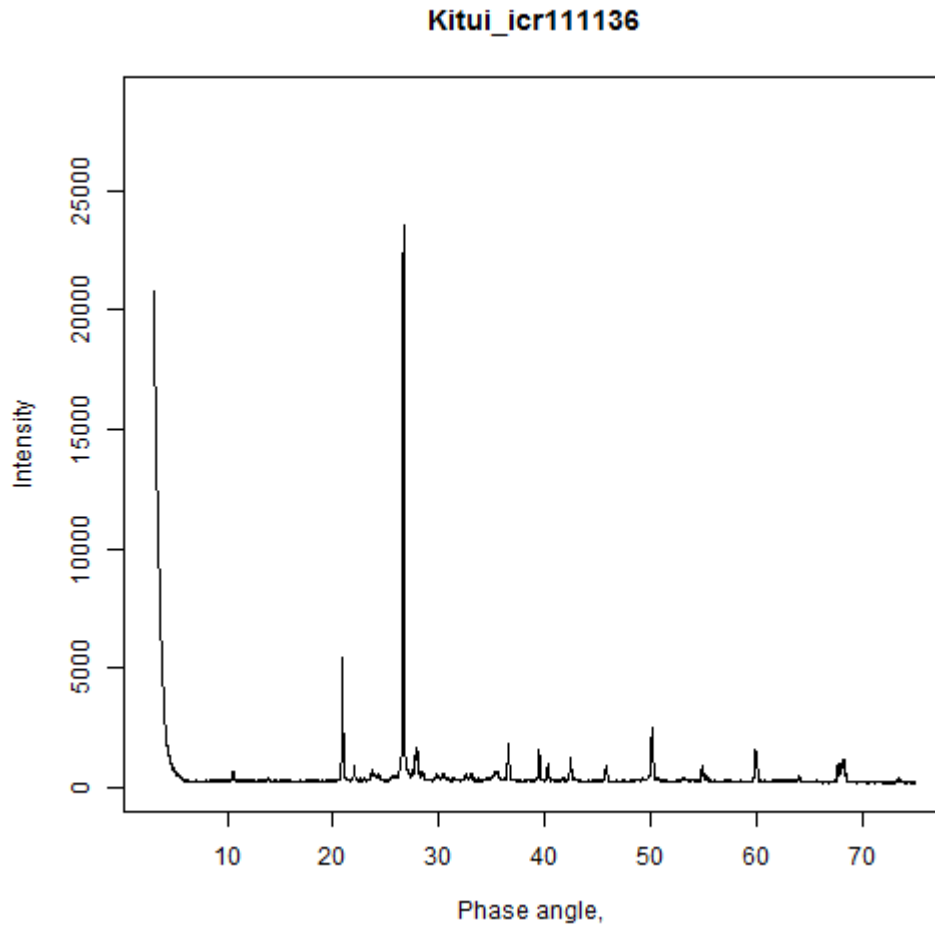
Figure 1: XRD spectrum for sample 2

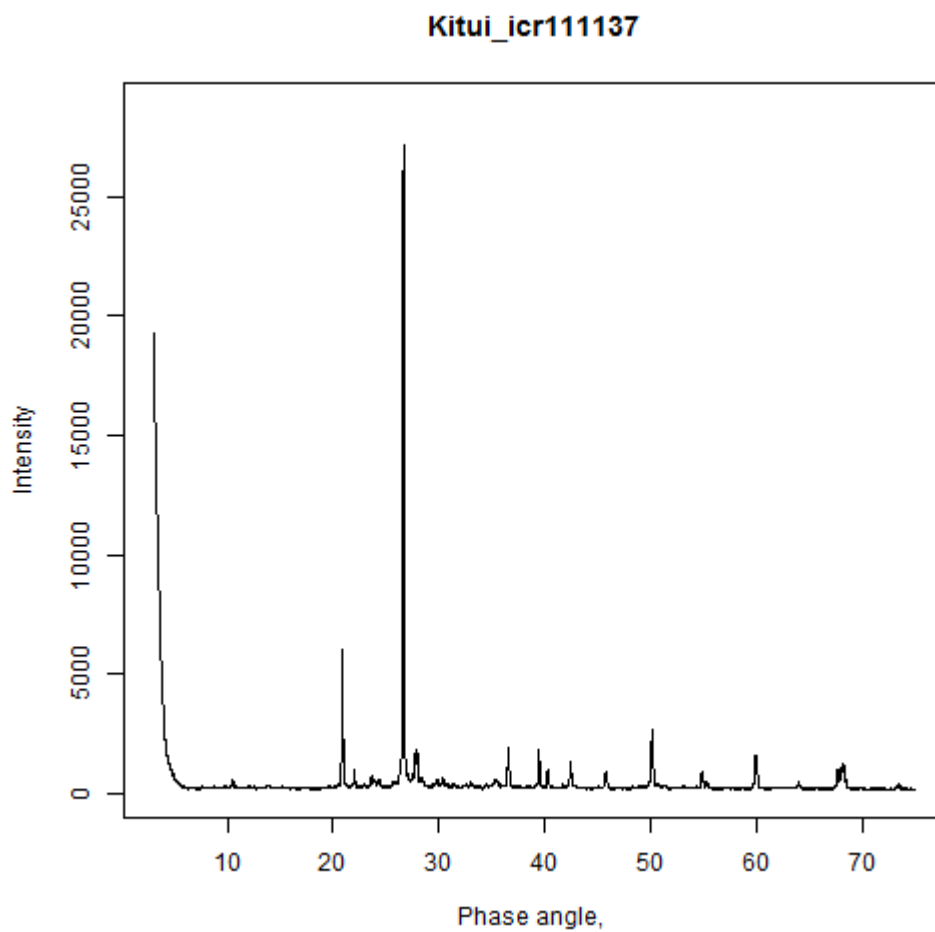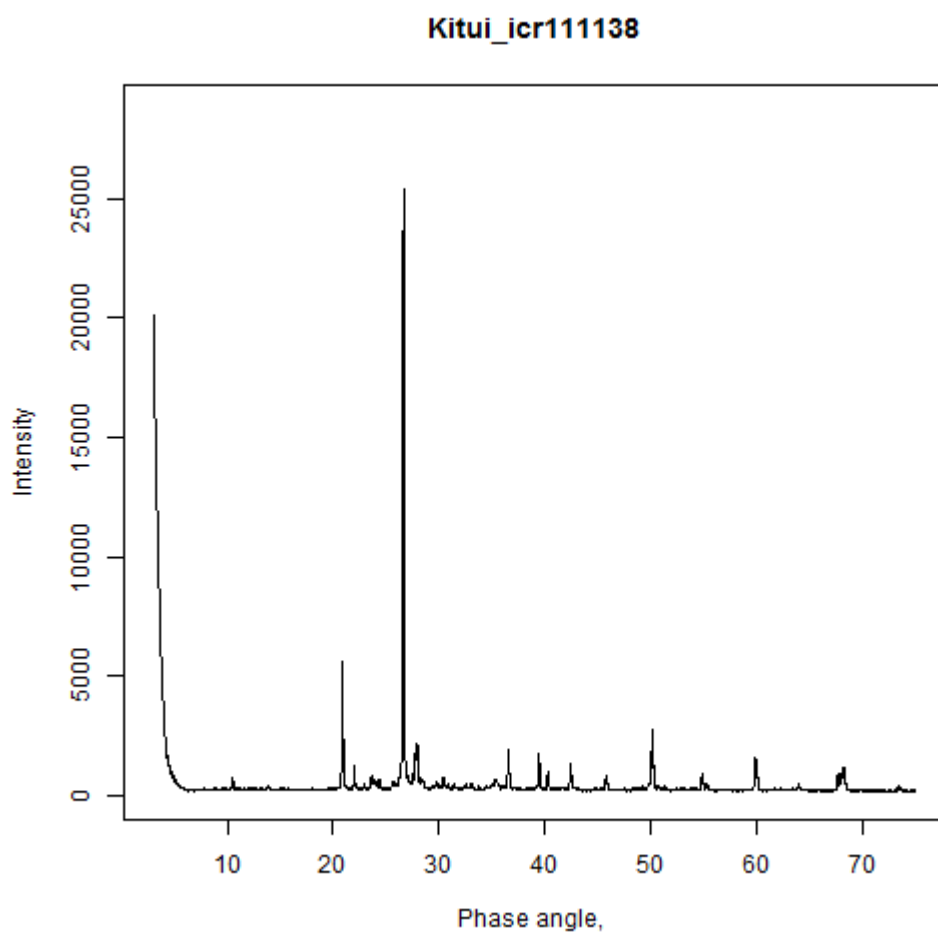**Figure 2: XRD Spectrum for sample 6**

Kitui_icr111138

Figure 3: XRD spectrum for sample 7
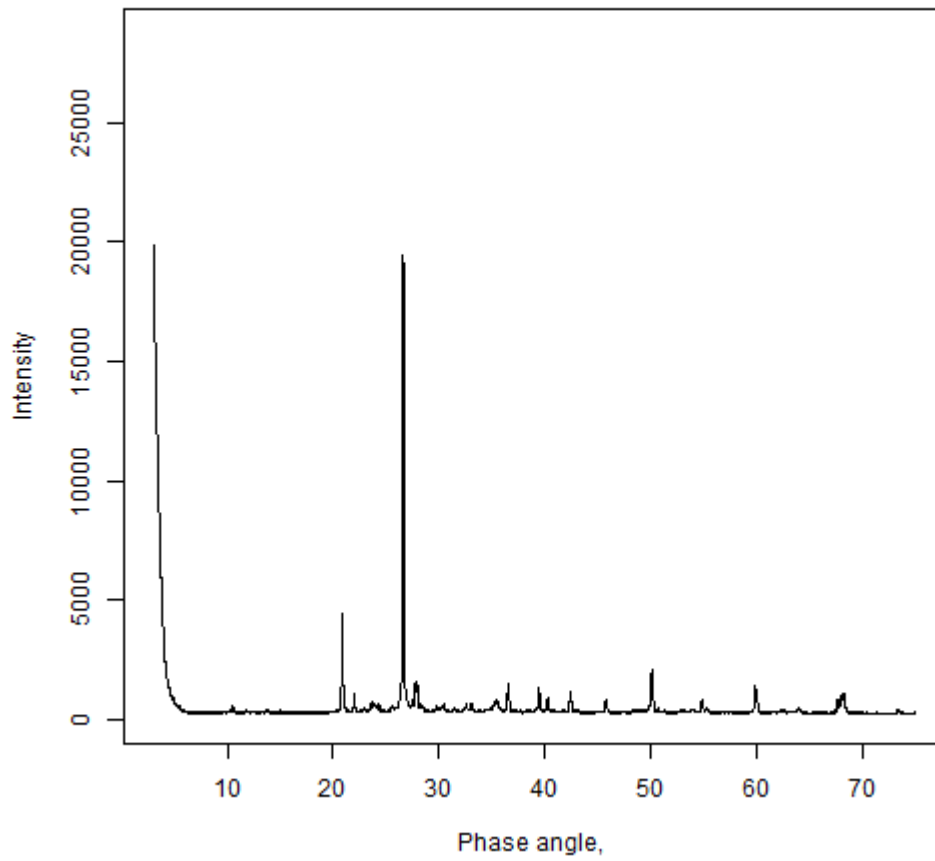
Figure 4: XRD spectrum for sample 12

Kitui_icr111140
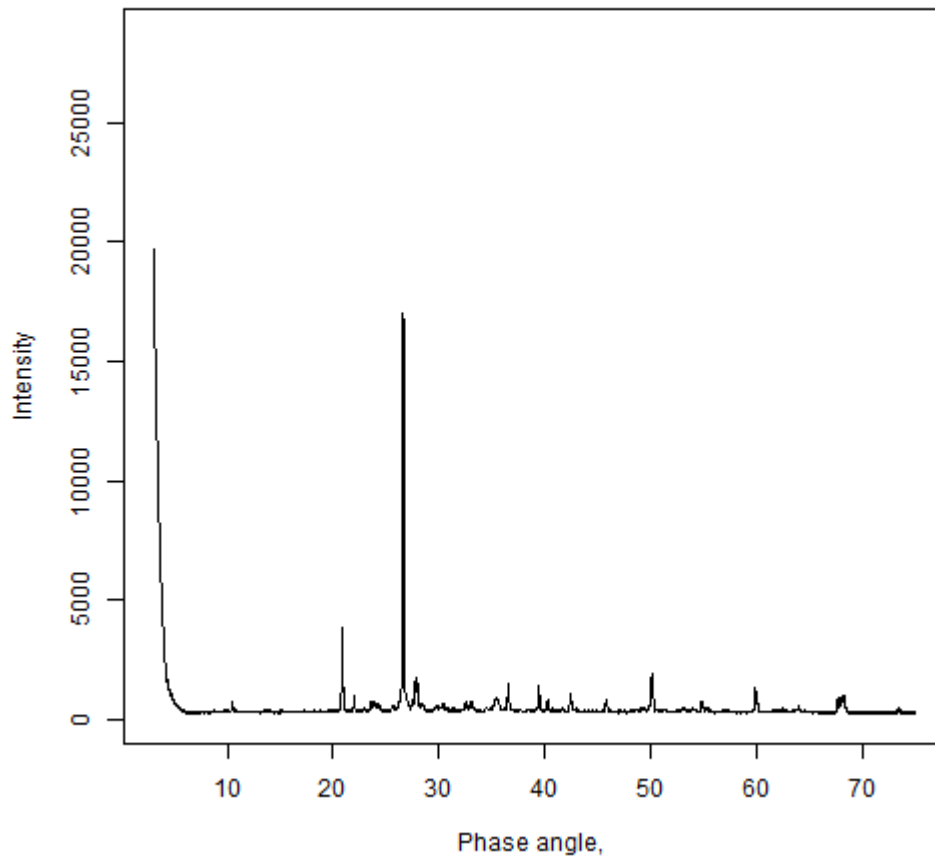
Figure 5: XRD Spectrum for sample 13
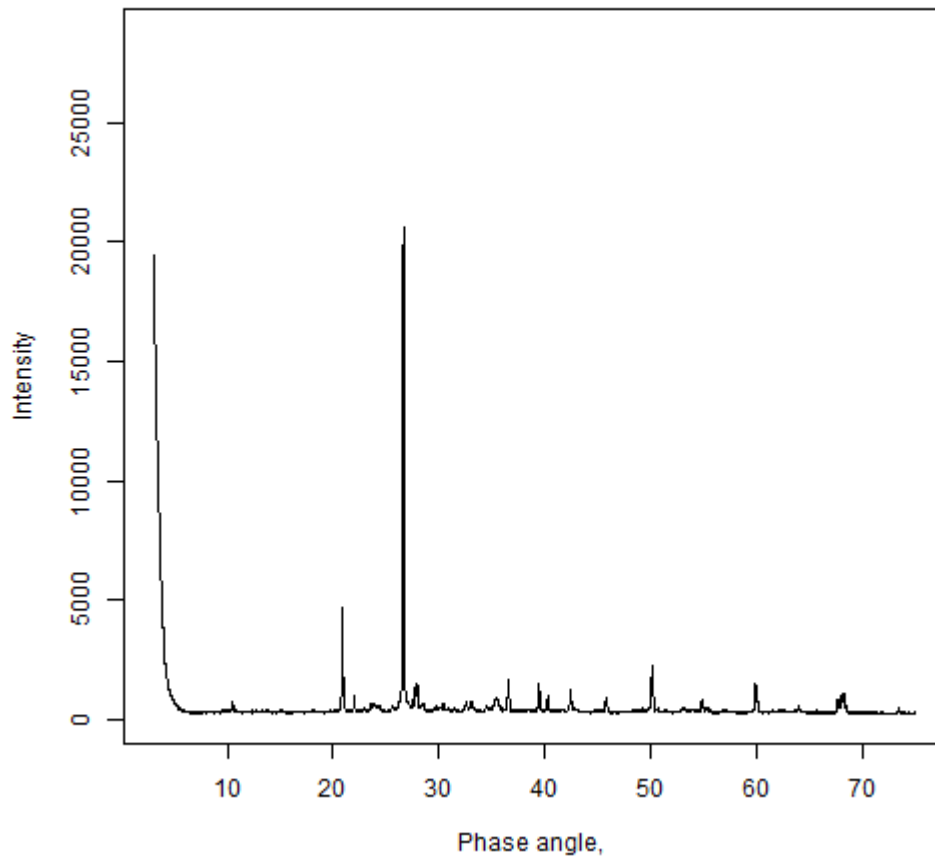
Figure 6: XRD Spectrum for sample 16
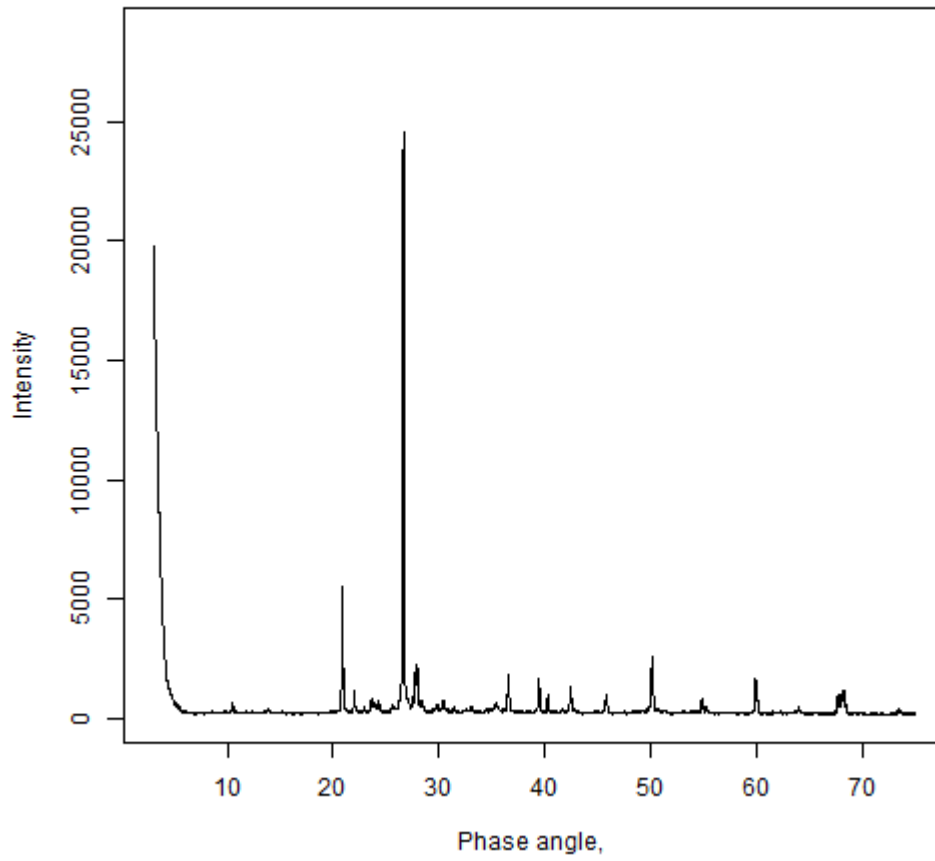
Kitui_icr111142
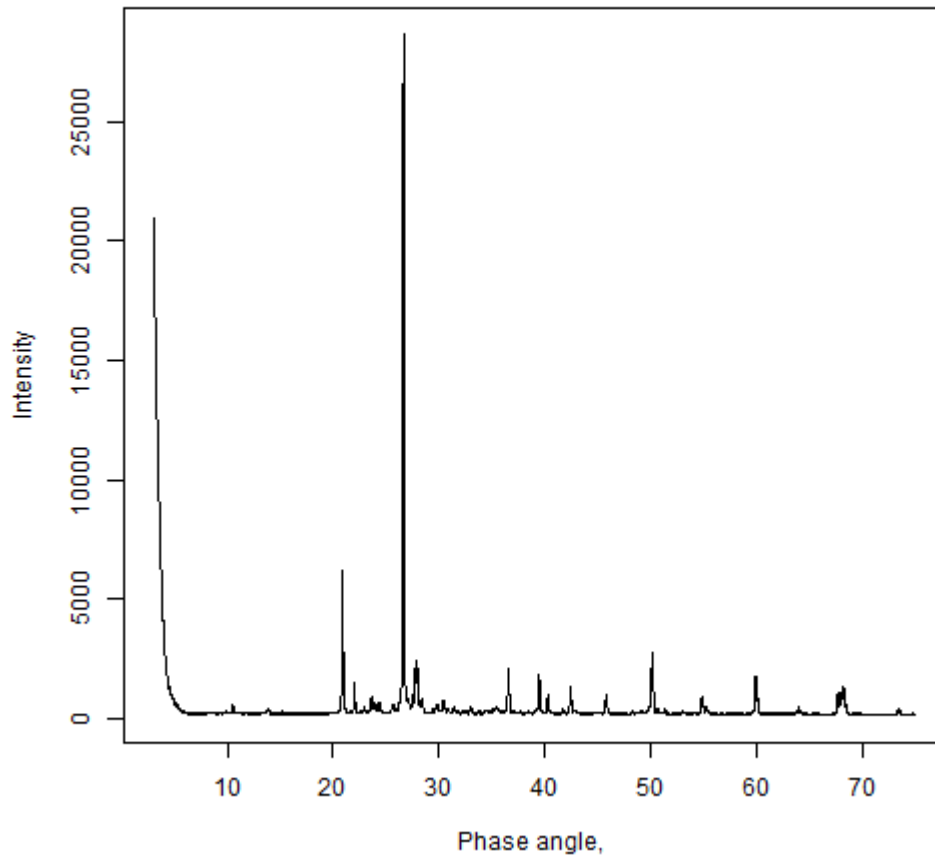
Figure 7: XRD Spectrum for sample 20a

Figure 8: XRD Spectrum for sample 22b
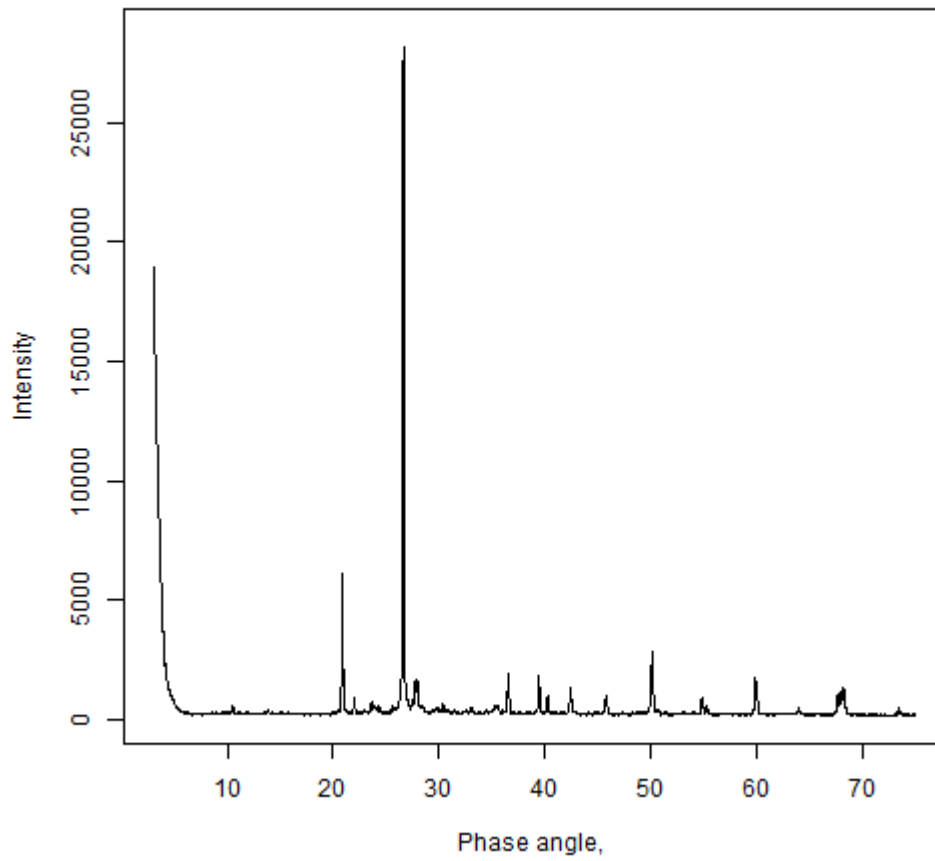
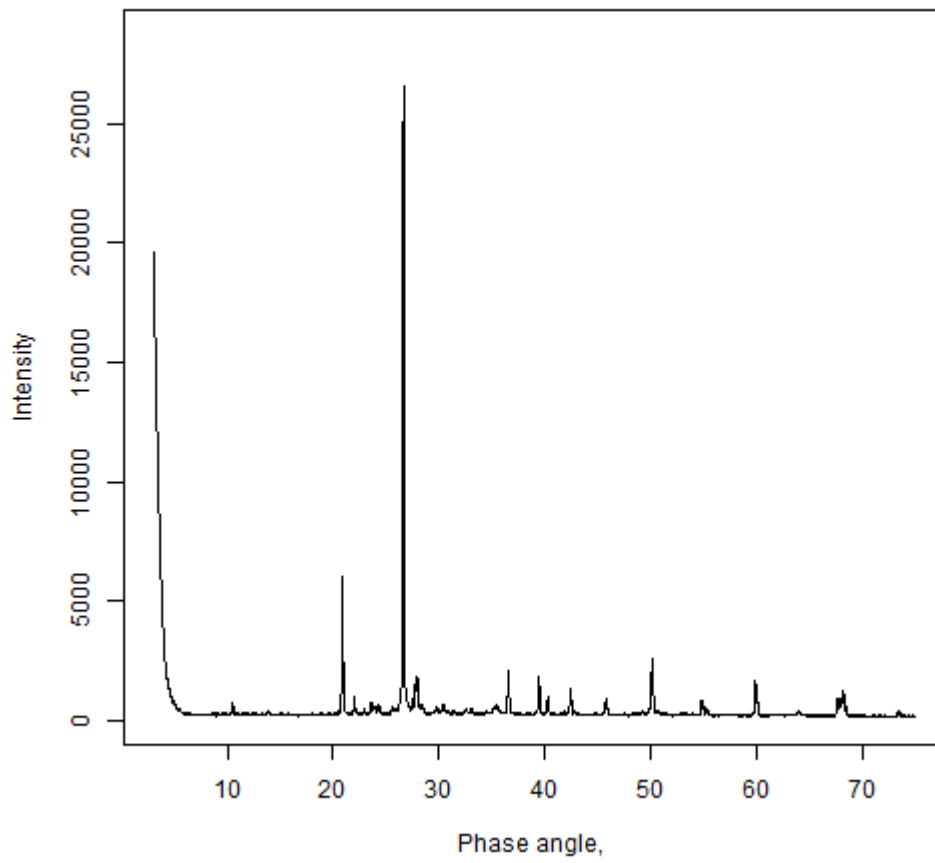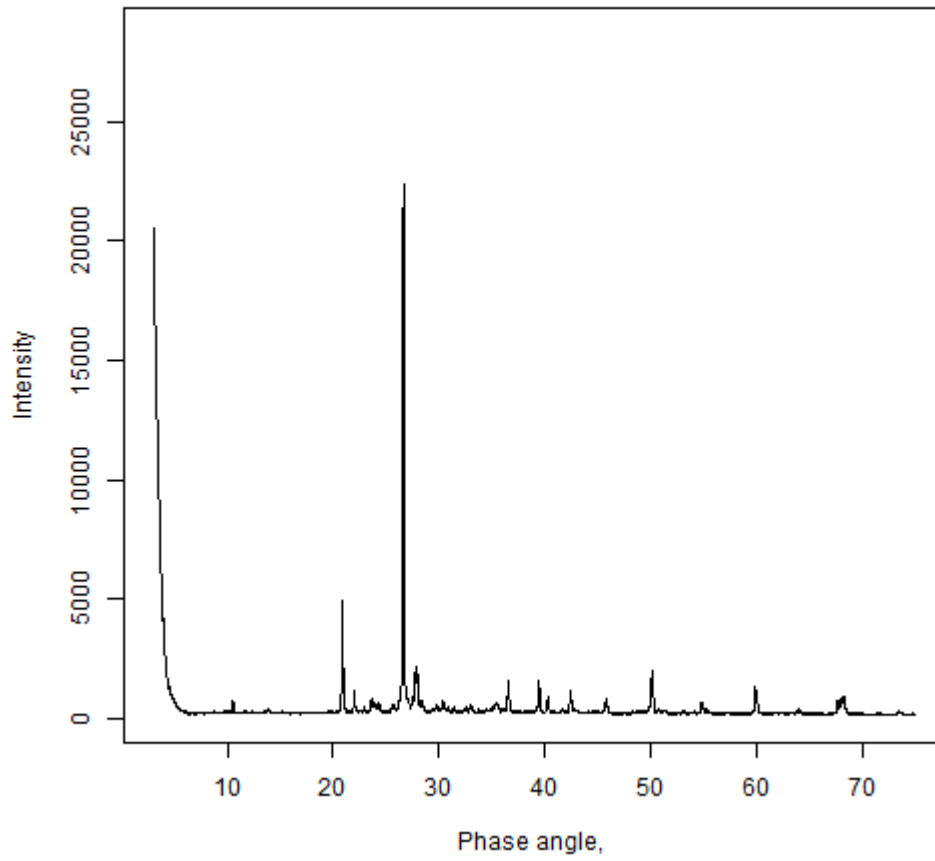**Figure 9: XRD spectrum for sample 27**

Figure 10: XRD Spectrum for sample 27

Kitui_icr111147

Figure 11: XRD Spectrum sample 29